Lawrence Berkeley National Laboratory
LBL Publications

Title
Measured temperature reductions and energy savings from a cool tile roof on a central California home

Permalink
https://escholarship.org/uc/item/46s7041c

Authors
Rosado, Pablo J.
Faulkner, David
Sullivan, Douglas P.
et al.

Publication Date
2014-09-01

ERNEST ORLANDO LAWRENCE
BERKELEY NATIONAL LABORATORY

Measured temperature reductions and energy savings from a cool tile roof on a central California home
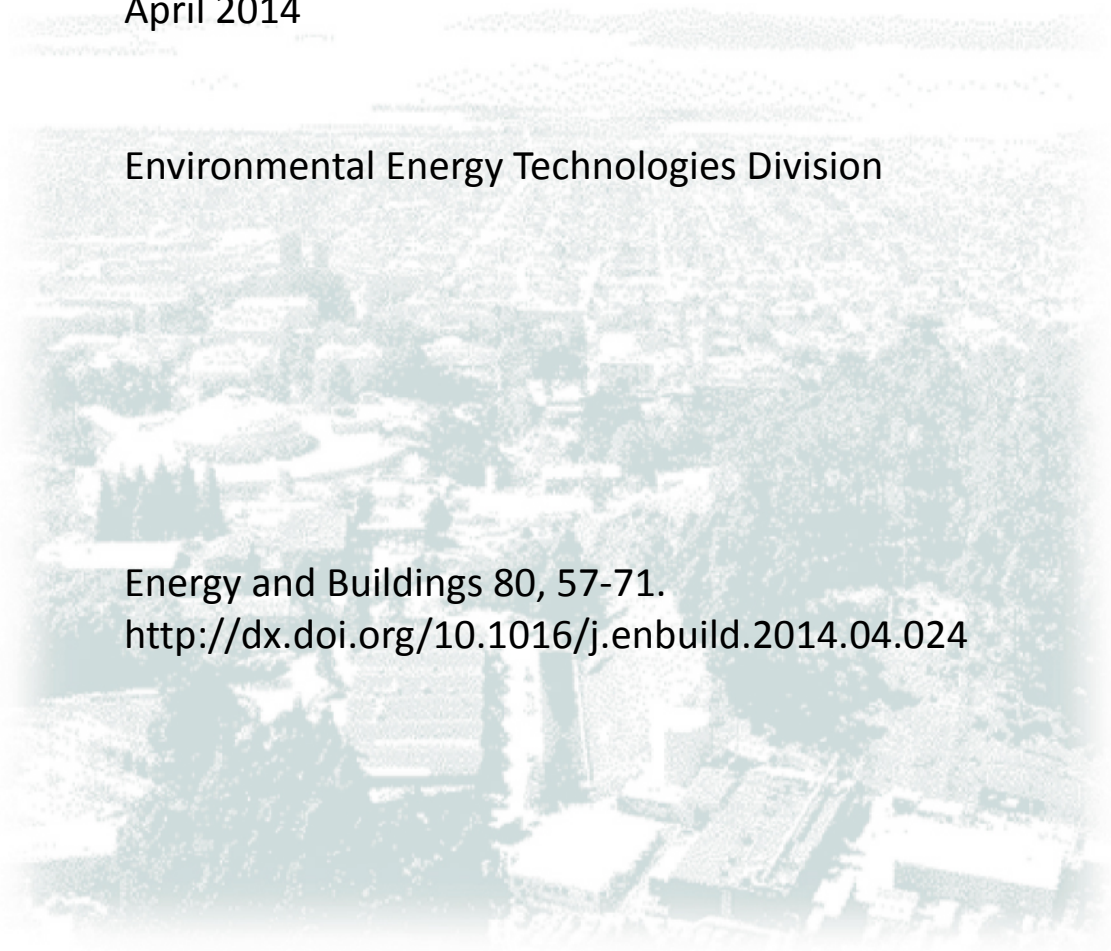
Pablo J. Rosado, David Faulkner, Douglas P. Sullivan, Ronnen Levinson

April 2014

Disclaimer

Acknowledgments

Measured temperature reductions and energy savings from a cool tile roof on a central California home

Pablo J. Rosado, David Faulkner, Douglas P. Sullivan, Ronnen Levinson*

Lawrence Berkeley National Laboratory, Berkeley, CA, United States

A B S T R A C T

To assess cool-roof benefits, the temperatures, heat flows, and energy uses in two similar single-family, single-story homes built side by side in Fresno, California were measured for a year. The "cool" house had a reflective cool concrete tile roof (initial albedo 0.51) with above-sheathing ventilation, and nearly twice the thermal capacitance of the standard dark asphalt shingle roof (initial albedo 0.07) on the "standard" house.

Cool-roof energy savings in the cooling and heating seasons were computed two ways. Method A divides by HVAC efficiency the difference (standard − cool) in ceiling + duct heat gain. Method B measures the difference in HVAC energy use, corrected for differences in plug and window heat gains.

Based on the more conservative Method B, annual cooling (compressor + fan), heating fuel, and heating fan site energy savings per unit ceiling area were $2.82\,kWh/m^2$ (26%), $1.13\,kWh/m^2$ (4%), and $0.0294\,kWh/m^2$ (3%), respectively. Annual space conditioning (heating + cooling) source energy savings were $10.7\,kWh/m^2$ (15%); annual energy cost savings were $0.886/m^2$ (20%). Annual conditioning CO_2, NO_x, and SO_2 emission reductions were $1.63\,kg/m^2$ (15%), $0.621\,g/m^2$ (10%), and $0.0462\,g/m^2$ (22%). Peak-hour cooling power demand reduction was $0.88\,W/m^2$ (37%).

© 2014 Elsevier B.V. All rights reserved.

1. Introduction

The number and size of air-conditioned homes in hot climates has risen significantly over the past 20 years, increasing U.S. residential cooled floor area by 71% [1]. Boosting the albedo (solar reflectance) of a building's roof can save cooling energy in summer by reducing solar heat gain, lowering roof temperature, and decreasing heat conduction into the conditioned space and the attic ducts. It may also increase the use of heating energy in winter. Prior research has indicated that net annual energy cost savings are greatest for buildings located in climates with long cooling seasons and short heating seasons, especially those buildings that have distribution ducts in the attic [2–7].

Solar-reflective "cool" roofs decrease summer afternoon peak demand for electricity [3,8,9], reducing strain on the electrical grid and thereby lessening the likelihood of brownouts and blackouts. Reducing peak cooling load can also allow the installation of a smaller, less expensive air conditioner. This is referred to as a "cooling equipment" saving [9]. Smaller air conditioners are also

typically less expensive to run, because air conditioners are more efficient near full load than at partial load.

Roofs can cover a substantial fraction of the urban surface. For example, when viewed from above the tree canopy, roofs comprise about 19–25% of each of four U.S. metropolitan areas—Chicago, IL; Houston, TX; Sacramento, CA; and Salt Lake City, UT [10]. Citywide installation of cool roofs can lower the average surface temperature, which in turn cools the outside air. A meta-analysis of meteorological simulations performed in many U.S. cities found that each 0.1 rise in urban albedo (mean solar reflectance of the entire city) decreases average outside air temperature by about 0.3 K, and lowers peak outside air temperature by 0.6–2.3 K [11]. Cool roofs thereby help mitigate the "daytime urban heat island" by making cities cooler in summer. This makes the city more habitable, and saves energy by decreasing the need for air conditioning in buildings. Cooler outside air can also improve air quality by slowing the temperature-dependent formation of smog [12,13].

Replacing a hot roof with a cool roof immediately reduces the flow of thermal radiation into the troposphere ("negative radiative forcing"), offsetting the global warming induced by emission of greenhouse gases [14–16]. Most recently, Akbari et al. [17] estimated that increasing by 0.01 the albedo of $1\,m^2$ of urban surface provides a one-time (not annual) offset of 4.9–12 kg CO_2. Substituting $100\,m^2$ of cool white roofing (albedo 0.6) for standard

gray roofing (albedo 0.2) would provide a one-time offset of about 20–48 t CO_2.

The direct cooling benefits of increasing the albedo of a residential roof have been simulated or measured by several workers. For example, Akbari et al. [3] simulated with the DOE-2 building energy model the annual cooling and heating energy uses of a variety of building prototypes in 11 U.S. cities. They found that raising the albedo of an RSI-3.3 asphalt-shingle roof by 0.30 reduced the annual cooling energy use of a single-story home by 6–15%, and increased annual heating energy use by 0–5%.

Parker and Barkaszi [18] measured daily cooling energy uses in summer before and after applying white roof coatings to nine single-story Florida homes. Savings ranged from 2 to 40% and averaged 19%. In a home with RSI-3.3 ceiling insulation, increasing the albedo of an asphalt shingle roof by 0.44 (to 0.59 from 0.15) reduced daily cooling energy use by 10%, and lowered peak cooling power demand by 16%.

Miller et al. [19] measured cooling energy uses in three pairs of Northern California homes. Each pair of homes had color-matched standard (lower albedo) and cool (higher albedo) roofs. The first pair had brown concrete tile roofs with albedos of 0.10 (standard) and 0.40 (cool); the second, brown metal roofs with albedos of 0.08 (standard) and 0.31 (cool); and the third, gray-brown shingle roofs with albedos of 0.09 (standard) and 0.26 (cool). After adjusting for widely disparate occupancy patterns, summer daily cooling energy savings were estimated to be about 9% in the homes with the cool tile and cool metal roofs; savings for the cool shingle roof were unclear.

High thermal capacitance and/or subsurface natural convection ("above-sheathing ventilation") in the roof system can further cool the building [20–23]. For example, Miller and Kosny [24] measured the summer daily heat flows through an SR 0.13 flat tile roof on double battens and through an SR 0.09 shingle roof, each installed over a modestly insulated (RSI-0.9) ceiling in a test assembly. The heat flow through the tile roof was only half that through the shingle roof, even though the solar absorptance (1 – solar reflectance) of the tile was only 4% lower than that of the shingle. Note that above-sheathing ventilation (air flow in the space between sheathing, or roof deck, and the roofing product) is usually driven by buoyancy, rather than wind, because building codes typically require the air space at the eave (bottom edge) of the roof to be closed for fire protection [25].

Two of the most popular roofing product categories in the western U.S. residential roofing market are fiberglass asphalt shingles (hereafter, "shingles") and clay or concrete tiles (hereafter, "tiles"). Surveys by *Western Roofing Insulation & Siding* found that shingles and tiles comprised 50% and 27% of 2007 sales, respectively, and 63% and 14% of projected 2013 sales [26,27]. Substituting a light-colored tile for a dark asphalt shingle reduces the roof's solar heat gain, roughly doubles its thermal capacitance [28], and provides above-sheathing ventilation. In a mild-winter climate where heating is needed primarily in the morning, this substitution may even decrease heating energy use in winter. This is possible because increasing the roof's thermal capacitance keeps the attic warmer overnight, while high roof albedo has little consequence after sunset.

The present study compares two side-by-side, single-story, single-family houses in Fresno, California. Fresno is located in the state's Central Valley, a hot climate in which homes use air conditioning from approximately May to October. The first house has a standard dark asphalt shingle roof, and the second a cool concrete tile roof; they are otherwise quite similar in construction and use. The homes serve as show models and are open to the public every day from 09:00 to 17:00 local time (LT). By monitoring temperatures, heat flows, and energy consumption in these air-conditioned houses, we investigate the extents to which over the course of a year the cool roof reduces (a) roof and attic temperatures; (b) conduction of heat into the conditioned space and into HVAC ducts in the attic; (c) cooling and heating energy uses; and (d) peak-hour power demand. We also compare measured cooling energy savings to cooling energy savings calculated from heat flow and temperature measurements, in order to evaluate whether a simplified experimental configuration without power meters can be used in future cool roof experiments.

2. Theory

While the tested homes share similar floor and elevation plans, differences other than roof construction, such as those in plug load (appliances and lights), fenestration (window area, orientation, construction, and coverings), and occupancy, can influence building conditioning energy use. Here, we derive two ways to isolate the energy savings attributable to the cool roof.

2.1. Heat balance

The conditioned space (hereafter, "room") can gain or lose heat through its envelope (ceiling, walls, floor, and windows), and gain heat from internal sources, including plug loads (appliances and lighting) and people. Conditioned air can also gain or lose heat as it flows through the attic ductwork from the air conditioner or furnace to the room. Denoting the rates of heat gain (power) in the room and ductwork as q_{room} and q_{duct}, the building's combined heat load is

$$q_{load} \equiv q_{room} + q_{duct}. \tag{1}$$

The rate q_{HVAC} at which the furnace or air conditioner must remove heat to regulate room air temperature (positive in the cooling season, negative in the heating season) is

$$q_{HVAC} = q_{load}. \tag{2}$$

We disaggregate q_{room} into gains from the ceiling, plug load, windows, and other sources (e.g., walls, floor, infiltration and occupants), such that

$$q_{room} = q_{ceiling} + q_{plug} + q_{window} + q_{other}. \tag{3}$$

The rate of heat gain through the ceiling, $q_{ceiling}$, is the product of ceiling area and ceiling heat flux (power/area). The rate of plug load heat gain, q_{plug}, equals the plug load electric power demand. The rate of heat gain through the windows, q_{window}, can be estimated from solar irradiance and the area, construction, orientation, and coverings of windows.

The rate of heat gain through attic ductwork is

$$q_{duct} = \dot{m}c_p[\delta T_{supply} + \delta T_{return}] \tag{4}$$

where $\dot{m}$ and c_p are the mass flow rate and specific heat capacity of the duct air, δT_{supply} is the temperate rise (outlet – inlet) along the supply duct, and δT_{return} is the temperature rise along the return duct. Note that neglecting minor thermal storage in the duct work, duct heat gain vanishes when the HVAC system is off ($\dot{m} = 0$). If duct air temperature rises have not been measured, q_{duct} can be estimated as

$$q_{duct} = \bar{U}A_{duct} \frac{\theta_{out} - \theta_{in}}{\ln(\theta_{out}/\theta_{in})} \tag{5}$$

where $\bar{U}$ is the thermal transmittance of the duct wall, A_{duct} is duct surface area, inlet temperature depression $\theta_{in} = T_{attic\ air} - T_{inlet}$, and outlet temperature depression $\theta_{out} = T_{attic\ air} - T_{outlet}$ [29]. In the supply duct, T_{inlet} can be estimated from room air temperature and HVAC equipment specifications of temperature drop across the evaporator (often approximately 10 °C) and temperature rise across

the furnace; in the return duct, T_{inlet} can be approximated by room air temperature. Air temperature at the outlet of either duct can be estimated from

$$\frac{T_{outlet} - T_{attic\,air}}{T_{inlet} - T_{attic\,air}} = \exp\left(-\frac{\bar{U}A_{duct}}{\dot{m}c_p}\right). \tag{6}$$

The rate of HVAC heat removal during the cooling season is

$$q_{cooling} \equiv q_{HVAC,\,cooling} = C \times P_{cooling} \tag{7}$$

where C is the coefficient of performance (COP) of the cooling equipment (compressor and fan) and $P_{cooling}$ is its electric power demand. Similarly, the rate of HVAC heat removal in the heating season is

$$q_{heating} \equiv q_{HVAC,\,heating} = -\eta \times P_{heating} \tag{8}$$

where η is the annual fuel utilization efficiency (AFUE) of the furnace and $P_{heating}$ is its rate of fuel energy consumption. Note that while $P_{cooling}$ includes electric fan power, $P_{heating}$ does not.

COP can be computed from seasonal energy efficiency ratio (SEER) by applying the SEER-to-EER conversion given by Hendron and Engebrecht [30] and the unit conversion EER = COP × 3.412 BTU/Wh to obtain

$$C = \frac{-0.02 \times SEER^2 + 1.12 \times SEER}{3.412}. \tag{9}$$

2.2. Energy savings

Consider two buildings, one with a standard roof and the other with a cool roof, that are otherwise matched in size and shape, and in particular have the same ceiling and duct areas. Defining $\Delta x \equiv x_{standard} - x_{cool}$,

$$\Delta q_{HVAC} = \Delta q_{load}. \tag{10}$$

The difference in heat load can be disaggregated as

$$\Delta q_{load} = \Delta q_{room} + \Delta q_{duct} = \Delta q_{ceiling} + \Delta q_{plug} + \Delta q_{window} + \Delta q_{other} + \Delta q_{duct}. \tag{11}$$

If the duct wall is well insulated, or the duct air flow rate is high, the air temperature drop from inlet to outlet of each duct will be small. This can be tested by checking whether the expression on the right hand side of Eq. (6) is close to unity. If further (a) the supply ducts in each building share the same inlet temperature, wall thermal transmittance, and wall area; (b) the same is true of the return ducts; and (c) both HVAC systems are on, then it follows from Eq. (5) that

$$\Delta q_{duct,\,supply} = \bar{U}_{supply} A_{supply} \Delta T_{attic\,air} \tag{12}$$

and

$$\Delta q_{duct,\,return} = \bar{U}_{return} A_{return} \Delta T_{attic\,air} \tag{13}$$

This permits estimation of $\Delta q_{duct} = \Delta q_{duct,\,supply} + \Delta q_{duct,\,return}$ without measuring or calculating duct inlet and outlet temperatures.

If the buildings' HVAC systems share the same COP C and AFUE η, then

$$\Delta q_{cooling} = C \times \Delta P_{cooling} \tag{14}$$

and

$$\Delta q_{heating} = -\eta \times \Delta P_{heating}. \tag{15}$$

The HVAC power savings (standard building – cool building) in the cooling and heating seasons are

$$\Delta P_{cooling} = \frac{\Delta q_{cooling}}{C} = \frac{\Delta q_{load}}{C} \tag{16}$$

and

$$\Delta P_{heating} = \frac{-\Delta q_{heating}}{\eta} = \frac{-\Delta q_{load}}{\eta} \tag{17}$$

respectively.

To distinguish conditioning power savings attributable to the roof from those that result from differences in plug, window, or other heat loads, we define the cool-roof cooling power savings in the cooling season as

$$\Delta P_{cooling,\,roof} \equiv \frac{\Delta q_{ceiling} + \Delta q_{duct}}{C} \tag{18}$$

and the cool-roof heating power savings in the heating season (potentially negative) as

$$\Delta P_{heating,\,roof} \equiv -\frac{\Delta q_{ceiling} + \Delta q_{duct}}{\eta}. \tag{19}$$

This first approach—"Method A"—estimates cool-roof cooling and heating power savings from measured ceiling heat gain and calculated duct heat gain.

Our second approach—"Method B"—calculates cool-roof cooling and heating power savings from measured HVAC power savings after correcting for differences in plug, window, and other heat loads. If $\Delta q_{other} = 0$, combining Eqs. (11), (16) and (18) yields the cooling (compressor + fan) power savings attributable to the cool roof,

$$\Delta P_{cooling,\,roof} = \Delta P_{cooling} - \frac{\Delta q_{plug} + \Delta q_{window}}{C} \tag{20}$$

while combining Eqs. (11), (17) and (19) yields the heating fuel energy savings rate attributable to the cool roof,

$$\Delta P_{heating,\,roof} = \Delta P_{heating} + \frac{\Delta q_{plug} + \Delta q_{window}}{\eta} \tag{21}$$

Since $P_{heating}$ excludes electric fan power, and AFUE η also neglects fan power, neither method includes cool-roof fan power savings in the heating season. We estimate this value as

$$\Delta P_{fan,\,heating,\,roof} = \Delta P_{fan,\,heating} \times \frac{\overline{\Delta P_{heating,roof}}}{\overline{\Delta P_{heating}}} \tag{22}$$

where bar denotes mean over the heating season.

If the envelope of each home is well insulated, room heat gains (or losses) that occur while the HVAC system is off will warm or cool the room's surfaces and air, influencing the conditioning load when the HVAC system later operates. Therefore, daily, cooling season, and heating season site energy savings are each evaluated by integrating power savings over all hours in the day or season, including those times in which the HVAC system is off. That is, site energy savings are calculated as

$$\Delta E \equiv \int \Delta P \, dt. \tag{23}$$

This assumption appears safe in the cooling season, because the mid-morning period during which there is typically a substantial ceiling heat gain without HVAC operation is immediately followed by late-morning to early-evening HVAC operation. In the heating season, this assumption may overestimate cool-roof heating energy penalties, because the HVAC system operates primarily in the early morning, nearly 12 h after the sun has set and during a period in which the cool roof will have minimal impact on the attic/duct heat balance (Appendix A).

Cool-roof energy savings are assumed to be zero on days when HVAC systems are off in both homes.

2.3. Other savings

The following savings are all annual.

2.3.1. Source energy savings

If substituting a cool roof for a standard roof yields cooling (compressor + fan) site energy savings $\Delta E_{\text{cooling, roof}}$, heating fuel site energy savings $\Delta E_{\text{heating, roof}}$, and heating fan site energy savings $\Delta E_{\text{fan, heating, roof}}$, the source energy savings will be

$$\Delta s = r_e \left(\Delta E_{\text{cooling}} + \Delta E_{\text{fan, heating, roof}} \right) + r_g \Delta E_{\text{heating}} \qquad (24)$$

where r_e and r_g are the source-to-site energy ratios for electricity and natural gas, respectively.

2.3.2. Energy cost savings

The energy cost savings will be

$$\Delta c = d_e \left(\Delta E_{\text{cooling}} + \Delta E_{\text{fan, heating, roof}} \right) + d_g \Delta E_{\text{heating}} \qquad (25)$$

where d_e and d_g are the prices of electricity and natural gas, respectively.

2.3.3. Emission reduction

The reduction in emission of pollutant i will be

$$\Delta p_i = f_{e,i}(\Delta E_{\text{cooling}} + \Delta E_{\text{fan, heating, roof}})/\eta_t + f_{g,i} \Delta E_{\text{heating}} \qquad (26)$$

where $f_{e,i}$ is its electricity emission factor (mass of pollutant i per unit electricity supplied to the grid), $f_{g,i}$ is its natural gas emission factor (mass of pollutant i per unit gas energy consumed), and η_t is the grid's transmission efficiency.

2.3.4. Peak-hour power demand reduction

Utilities may define hours of peak electrical demand. For example, the California Public Utilities Commission classifies 12:00–18:00 LT, Monday–Friday, May–October as peak demand hours for nonresidential users [31]. The peak-hour demand reduction on a given day is the ratio of cooling energy saved during those hours to the time interval spanned.

3. Experiment

3.1. Overview

Temperatures, heat flows, and HVAC (compressor + fan) energy uses are compared over the course of 12 months in two adjacent and similar homes in California's Central Valley, one with a standard roof and the other with a cool roof. Monthly rates of natural gas use for heating are obtained from utility statements.

Cool roof energy savings in the cooling and heating seasons are computed via both Method A (difference in ceiling + duct heat gain, divided by COP or AFUE) and Method B (difference in HVAC energy use, corrected for differences in plug and window heat gains). Seasonal and annual site energy savings, source energy savings, energy cost savings, and emission reductions are calculated with local source-to-site energy ratios, energy prices, and emission factors. Peak-hour power demand reduction is also computed.

3.2. Construction

Two side-by-side, single-story, single-family homes built by Granville Homes in Fresno, CA in summer/fall 2010 have been made available for this study. Each building is oriented with its front door facing east and the length of the home running east–west. Hence, one side of each roof faces south and the other north, each at a pitch of about 20°. The houses are similar in floor plan (ESM Fig. C-1) and elevation plan (Fig. 1a), with the main difference being that one

has a standard roof ("standard home") and the other has a cool roof ("cool home"). The homes serve as show models and are open to the public every day from 09:00 to 17:00 LT. Lights and appliances are scheduled to turn on during business hours. Each home has additional plug loads drawn by a flat screen TV and a sound system, though the TV and sound system in the standard home were not operated in winter.

The standard home has an asphalt shingle roof (CertainTeed Autumn Blend) measured following ASTM Standard C1549 [32] to have an initial SR of 0.07 (Fig. 1b). Shingles are nailed or stapled on an underlayment covering the roof deck (ESM Fig. C-2a).

The cool home has a flat concrete tile roof (Eagle Roofing model 4258, CRRC PID 0918-0008) rated with initial SR 0.51 (Fig. 1b) and three-year-aged SR 0.47 [33].[1] Each row of flat tiles rests on a horizontal batten and on a lower row of tiles, allowing air to circulate between the tiles and underlayment (ESM Fig. C-2b). Air enters at the eave and is exhausted at the ridge.

Based on CRRC-reported measurements for the tile product, and CRRC-reported measurements for comparable asphalt shingle products, the initial thermal emittance of each roof was about 0.9.

The homes are built with the AC compressor placed at the back of the house next to the wall, facing west; the furnace and ventilation fan are placed in the attic, approximately at the center of the floor plan. The ducts (RSI-1.1) run through a prefabricated truss support system located in the attic, supplying every room of the home. Each home is also equipped with a return grill, located outside the master bedroom. For attic ventilation, squared static gable vents are located on the west side of both attics, facing the backyard. Eave and profile-specific attic vents (O'Hagin's Inc., Rohnert Park, CA) provide additional attic ventilation. Each attic floor is covered with blown cellulose insulation of thermal resistance 3.3 m^2 K W^{-1} (RSI-3.3) [19 ft^2 °F h BTU^{-1} (R-19)].[2] Wall insulation is also RSI-3.3 (R-19), and the ventilation duct insulation is RSI-1.1 (R-6). Windows are double-paned.

Each home has a SEER-14 (~COP 3.5) air conditioner and an AFUE 92% gas furnace. ESM Table C-1 further details each home's roof, attic, envelope, and HVAC system.

3.3. Instrumentation and data acquisition

Sensors and dataloggers were installed between 27 August and 14 December 2010. Each home has been instrumented to measure external and internal temperatures, ceiling heat flux, and electricity use, while a roof-mounted station on the standard house records weather.

On a clear summer day in Fresno, the south face of a 20° pitch roof receives more direct solar irradiance than the north face at mid-day, when the sun is south–southeast to south–southwest, but less irradiance in the early morning (sun east–northeast) and early evening (sun west–northwest). On a clear winter day, the south face receives more direct irradiance all day, because the sun stays in the southern hemisphere (ESM Fig. C-3). For example, at solar noon on the summer solstice (June 21), when the solar altitude is 77°, the north face of a 20° tilt roof receives 16% less direct sunlight than the south face. At solar noon on the winter solstice (solar altitude 30°), the north face receives 78% less direct sunlight than the south

---

[1] The albedos reported for each roofing product are beam-normal, air mass 1.5 solar reflectance outputs of a Devices & Services Solar Spectrum Reflectometer. Because this metric tends to overestimate the solar reflectance of spectrally selective surfaces, the true albedo of the cool tile roof is likely 0.03–0.05 lower than rated [34,35].

[2] Attic insulation thermal resistance was chosen to represent median-age housing stock, rather than new construction. In 2011, the median year of construction for homes in the U.S. Pacific census division (California, Oregon, Washington, Hawaii, and Alaska) was 1976 [36].
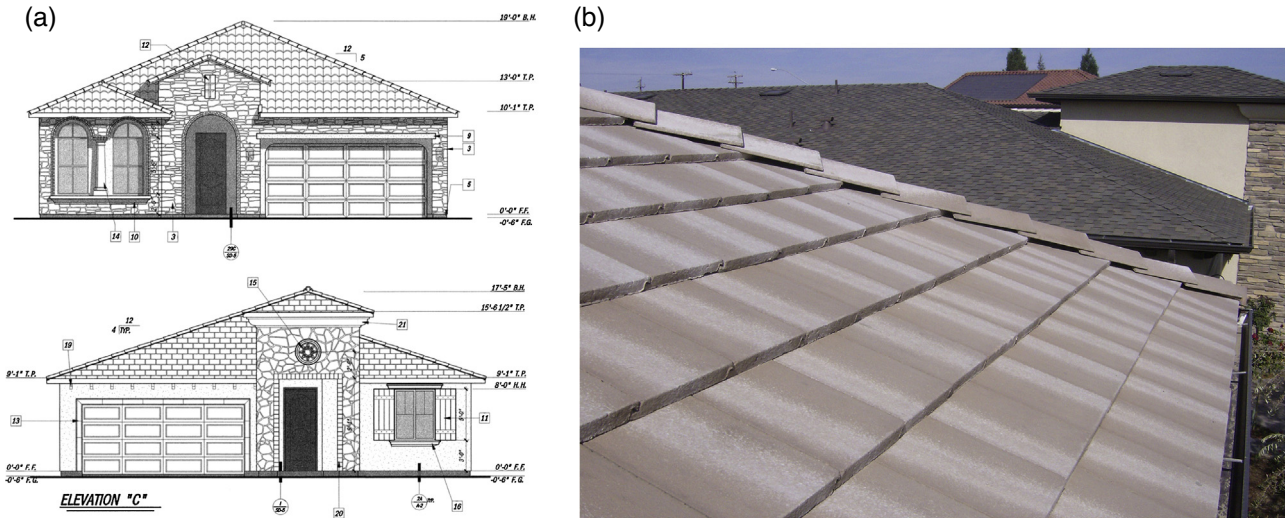
Fig. 1. Plans and image of adjacent single-family homes in Fresno, CA, showing (a) elevations of homes with cool roof (top) and standard roof (bottom); and (b) cool concrete tile roof (foreground) and standard asphalt shingle roof (background).

face [37]. Since this can make the north face of the roof cooler than the south face, sensors were placed on both the north and south sides of each house to assess building temperatures, and to explore the downward propagation of north-south temperature differences (Appendix B).

ESM Table C-2 summarizes the type and location of all sensors installed.

3.3.1. Roof

To measure the roof top temperature of the standard home, a thermistor was placed under a shingle on each side of the house (north and south), approximately at the center of each side (Fig. 2a). On the cool home the roof top temperature was measured with a thermistor placed near the upper surface of a tile on each side of the roof (Fig. 2b). To do so, a small hole was drilled at the back of the tile extending nearly to the top of the tile; the thermistor was embedded and epoxied inside this hole. This shielded the sensor from direct sunlight, wind, and outside air.

3.3.2. Attic

Each attic was instrumented with vertical arrays of thermistors on both the north and south side. On each side, one sensor was attached to the underside of the roof deck to measure the roof bottom, a second was suspended at mid-attic height, and a third was attached to the attic floor (Fig. 2). This vertical array of temperature

sensors was positioned mid-way along the home's east–west axis. To measure heat flux through the ceiling, a heat flux sensor was placed below the attic insulation and taped to the attic floor, near the south-side thermistor.

3.3.3. Room

Inside each home are two sensors, each of which measures both temperature and relative humidity. These are located at ceiling level near the ceiling-mounted return grill. Two additional thermistors were installed inside of each home. One was placed on the ceiling's surface below the heat flux sensor, and the other next to the thermostat of the HVAC system. The latter is used to measure room air temperature.

3.3.4. Weather station

A weather station was mounted on a tower fixed at the top of the west end wall of the standard home, and extends 1.5 m above roof line. The tower has a combined and self-contained temperature and relative humidity transmitter. The sensors of the transmitter are shielded by a cylindrical PVC rain and sun guard to prevent wetting of the humidity sensor and keep direct sunlight from shining on the sensors. A three-cup anemometer and a precision potentiometric wind vane are mounted at the top of the tower. A blue-enhanced photodiode pyranometer was also installed at the top of the tower to measure global horizontal solar irradiance.
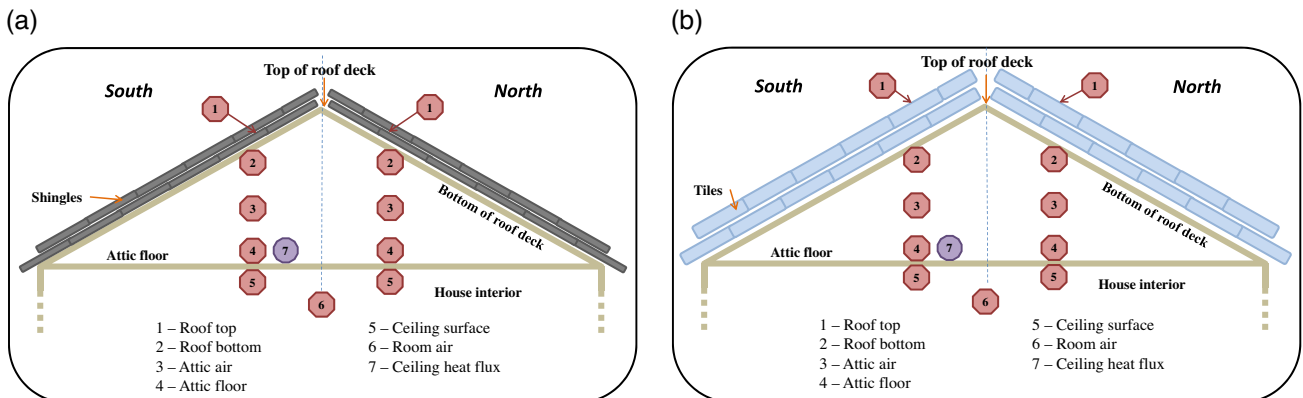

Fig. 2. Temperature and heat flux sensor locations in (a) the standard home and (b) the cool home.

3.3.5. Electric power monitoring devices

Three split-core current transformers (accuracy ±1%) were connected to the power meter of each home, measuring currents drawn by the AC compressor, ventilation fan, and entire house. The transformers are directly connected to a digital energy meter which reports power demand.

3.3.6. Data acquisition system

Two data loggers, one in each home, were used to acquire measurements. Each one has a multiplexer to increase the number of inputs. The data loggers are connected to the Internet for data transfer. They are both located in the master bedroom walk-in closet, inside the panel that contains the Internet wiring for each home. The data loggers are programmed to scan instantaneous readings every 30 s; data are transmitted hourly.

3.4. Estimation of window heat gain

Monthly window heat fluxes (energy/area) were evaluated with the Sustainable By Design window heat gain tool [38], using window solar heat gain coefficients (SHGCs) and orientations reported in building plans. The SHGC of each window and its covering (curtain or blind) was estimated using WINDOW software [39] assuming surface-normal solar incidence. Each monthly heat gain (energy per area) was then multiplied by window area and divided by its time interval (seconds in a month) to calculate its contribution to the rate of window heat gain, Q_{window} (power/area).

3.5. Building operation

From January to April 2011, the team tested the operation of the homes, the instrumentation and the retrieval of data. Measurements have been recorded and analyzed since May 2011, but in July 2011, the AC in the standard home started leaking refrigerant from a loose valve. This forced its compressor to overwork to satisfy the cooling demand. The problem was identified and addressed in April 2012 when an HVAC professional recharged the refrigerant in the standard home's AC, and verified that each home's AC was operating property.

During the 2012 cooling season (May–October), the thermostat in each home was set to 25 °C. During the 2012–2013 heating season (November–April), the thermostat in each home was set to 20 °C from 07:00 to 23:00 LT, and to 13 °C at other times.

3.6. Study period

This study analyzes nearly a full year of measurements collected from May 2012 through April 2013, during which time the HVAC system was monitored to ensure proper operation. About 7% of the data in this 12-month period—12 days in early January and 13 days in late April—was lost when communications were interrupted. In calculation of cumulative energy savings, daily energy savings for the 12 missing days in January are interpolated, while daily energy savings for the 13 missing days in late April are set to zero.

3.7. Local source-to-site energy ratios, energy prices, and emission factors

Method A and Method B site energy savings are converted to source energy savings and energy cost savings using the source-to-site energy ratios and site energy prices in Table 1. They are also converted to CO_2, NO_x, and SO_2 emission reductions using the emission factors in Table 2 and a grid transmission efficiency assumed to be 0.9.

Peak-hour demand reduction in the cooling season is calculated as the mean rate of cooling energy savings during peak-demand

Table 1

Source-to-site energy ratios and site energy prices in Fresno, CA.

	Electricity	Natural gas
Source-to-site energy ratio	3.34[a]	1.047[a]
Site energy price ($/kWh)	0.298[b]	0.0325[c]

[a] US average [43].
[b] Average Tier 3 (131–200% of baseline) electricity price in Fresno from March to October 2012 [44].
[c] Average Tier 1 (up to 100% of baseline) natural gas price in Fresno (November 2012–April 2013) [44], converted from $/therm at 29.3 kWh/therm.

Table 2

Year-2009 total and non-baseload output emission factors per unit electricity supplied to the grid in US EPA eGRID subregion WECC California [45], and non-regional natural gas combustion site emission factors per unit fuel energy consumed [46].

	CO_2 (kg/kWh)	NO_x (g/kWh)	SO_2 (g/kWh)
Total electricity	0.299	0.190	0.0826
Non-baseload electricity	0.451	0.146	0.0143
Natural gas	0.180	0.141	0.000887

hours, defined by the California Public Utilities Commission for nonresidential users as 12:00–18:00 LT, Monday–Friday, May–October [31]. We note that while the utility does not yet apply time-of-use rates to its residential customers, any peak-demand hour savings benefits the grid.

4. Results

4.1. Representative summer and winter days

4.1.1. Weather

6 July 2012 and 21 January 2013 were selected as representative sunny days in summer and winter, respectively. The maximum and minimum outside air temperatures on 6 July 2012 were similar to the average maximum and minimum values on July 6 from 1995 through 2011. However, the maximum outside air temperature on 21 January 2013 (sunny) exceeded the historical average for that day of year, because winter days in Fresno are often cloudy or rainy [40,41]. On the summer day, about 2 weeks after the summer solstice, outside air temperature ranged from 14.3 °C (04:53 local standard time [LST]) to 36.3 °C (15:14 LST); global horizontal solar irradiance peaked at 990 W/m² (12:07 LST), with 14.6 h from sunrise to sunset and 8.41 kWh/m² of solar irradiation. On the winter day, about 1 month after the winter solstice, outside air temperature ranged from 1.3 °C (06:05 LST) to 24.3 °C (14:16 LST); solar irradiance peaked at 578 W/m² (12:03 LST), with 10.1 h from sunrise to sunset and 3.45 kWh/m² of solar irradiation (Fig. 3).

4.1.2. Maximum building temperatures, ceiling heat gain, and duct heat gain

The cool home's higher roof albedo lowers its maximum attic air temperature, ceiling heat gain rate, and duct heat gain rate, which can reduce need for cooling energy in summer, and increase need for heating energy in winter.

For example, on the summer day, maximum roof top, roof bottom, and attic air temperatures in the cool home were 13.8, 14.3, and 10.5 °C lower than in the standard house. In the standard home, the roof top, roof bottom, and attic air temperatures reached their maxima at 12:42, 13:35, and 14:37 LST; in the cool home, the corresponding maxima were attained 68, 64, and 47 min later (Fig. 4a,b; ESM Table C-3). Maximum rates of ceiling, duct, and ceiling + duct heat gain in the cool home were 1.50, 0.89, and 2.4 kW lower than in the standard house (Fig. 5a; ESM Fig. C-4a,b; ESM Table C-3).

On the winter day, maximum roof top, roof bottom, and attic air temperatures in the cool home were 11.0, 10.6, and 6.9 °C lower
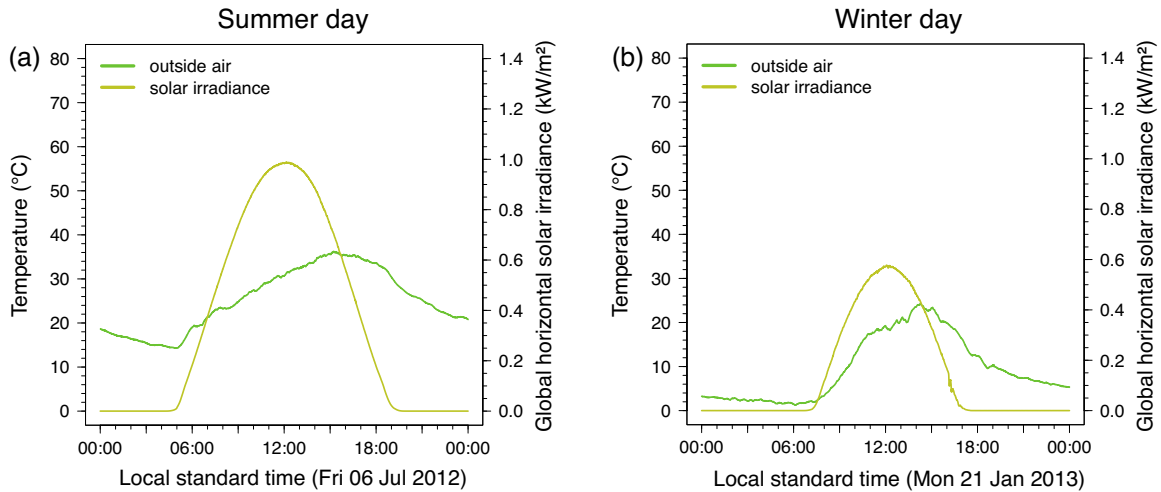
Fig. 3. Outside air temperature and global horizontal solar irradiance on (a) a sunny summer day (6 July 2012) and (b) a sunny winter day (21 January 2013).

than in the standard house. In the standard home, the roof top, roof bottom, and attic air temperatures reached their maxima at 13:06, 14:19, and 14:47 LST; in the cool home, the corresponding peaks were attained 65, 64, and 37 min later. Maximum ceiling, duct, and ceiling + duct rates of heat gain in the cool home were 0.83, 1.33, and 1.17 kW lower than in the standard house (Fig. 5b; ESM Fig. C-4c,d; ESM Table C-3).

On each day, the lags between peak temperatures in the cool and standard houses (e.g., time of roof top peak temperature in the cool house – time of roof top peak temperature in the standard house) are expected consequences of the higher thermal capacitance of the tile roof. Differences in maximum temperatures (standard – cool) are greater on the summer day than on the winter day because they occur in the afternoon, when there is more sunlight in summer than in winter. The same remarks also apply to ceiling temperatures.

4.1.3. Minimum building temperatures, ceiling heat gain, and duct heat gain

The cool home's higher roof thermal capacitance raises its minimum attic air temperature, ceiling heat gain rate, and duct heat gain rate, which can increase need for cooling energy in summer, and reduce need for heating energy in winter.

On the summer day, minimum roof top, roof bottom, and attic air temperatures in the cool home were 2.1, 2.4, and 2.4 °C *higher* than in the standard house; these minima were reached in the early morning, when cooling power demand is low. In the standard home, the roof top, roof bottom, and attic air temperatures reached their minima at 04:53, 05:09, and 05:17 LST; in the cool home, the corresponding minima were attained 14, 34, and 32 min later (Fig. 4a,b; ESM Table C-4). Minimum rates of ceiling, duct, and ceiling + duct heat gain in the cool home were 0.44, 0, and 0.44 kW *higher* than in the standard house (Fig. 5a; ESM Fig. C-4a,b; ESM Table C-4).

On the winter day, minimum roof top, roof bottom, and attic air temperatures in the cool home were 0.4, 2.1, and 2.3 °C *higher* than in the standard house. In the standard home, the roof top, roof, and attic air temperatures reached their minima at 05:15, 05:19, and 05:18 LST; in the cool home, the corresponding minima were attained 57, 21, and 24 min later. Minimum rates of ceiling, duct, and ceiling + duct heat gain in the cool home were 1.32, −0.12, and 1.20 kW *higher* than in the standard house (Fig. 5b; ESM Fig. C-4c,d; ESM Table C-4).

On each day, the minimum roof top, roof bottom, and attic air temperatures in the cool house are greater than those in the standard house because the tile roof is slower than the shingle roof

to cool to the outdoor air and night sky. The differences in minimum temperatures (cool – standard) on the summer day (2.1 to 2.4 °C) are comparable to those on the winter day (0.7 to 2.3 °C) because the minima occur long after sunset.

4.2. Daily solar irradiation and maximum outdoor air temperature

Clear-day global horizontal solar irradiation was up to three times greater in summer in Fresno than in winter, ranging from 2.9 kWh/m^2 (December) to 8.8 kWh/m^2 (June). Dips in daily solar irradiation indicate that cloudy days were more common in the heating season (November–April) than in the cooling season (May–October) (ESM Fig. C-5).

Clear-day maximum outdoor air temperature was up to 32 °C higher in summer than in winter, ranging from about 11 °C (December) to 43 °C (June) (ESM Fig. C-5).

4.3. Seasonal reductions in daily mean temperatures and heat gains

Seasonal mean reductions (standard – cool) in roof top, roof bottom, and attic air temperatures in the cooling season were about 3.4 °C, 3.7 °C, and 2.4 °C, roughly twice those in the heating season (Table 3). Ordinarily, one would expect to find the greatest temperature difference between standard (lower albedo) and cool (higher albedo) roofs at roof top, where sunlight is absorbed. In this experiment, above-sheathing ventilation cooling the deck of the cool tile roof may have made the temperature difference (standard – cool) at roof bottom (underside of roof deck) larger than that at roof top (just below tile surface). Daily maximum and mean roof top, roof bottom, and attic air temperatures are detailed in Fig. 6.

Cooling-season mean rates of ceiling and duct heat gain in the standard home were about 310 W and 130 W lower in the cool home than in the standard home. However, heating-season mean rates of ceiling and duct heat gain were about 46 W and 32 W *greater* in the cool home than in the standard home (Table 3). The higher heating-season mean ceiling and duct heat gains in the cool home are attributed to the higher thermal capacitance of the cool tile roof, which keeps the attic air under the cool roof warmer at night and early morning than that under the standard roof (Fig. 4f). In fact, the daily mean ceiling heat gain is greater in the cool house than in the standard house on most days between early November and late February, comprising two thirds of the heating season (ESM Fig. C-6a).
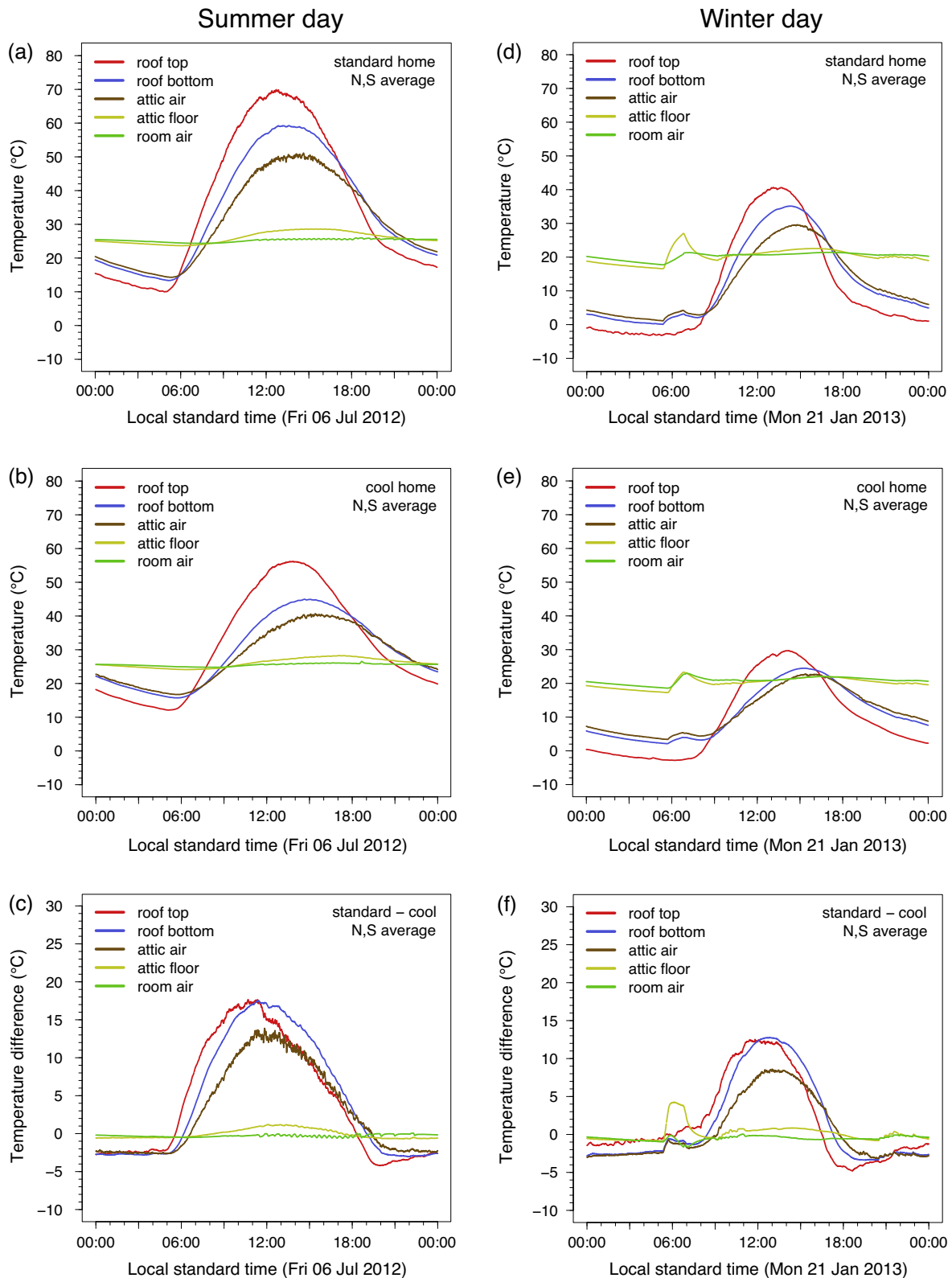
Summer day

Winter day

Fig. 4. Roof top, roof bottom, attic air, attic floor, and room air temperatures and temperature differences on (a–c) the summer day and (d–f) the winter day. Label "N,S average" applies to roof and attic temperatures.

Daily mean plug load heat gains were about the same in each house during the cooling season, but substantially higher in the cool house than in the standard house during the heating season, simply because the television and stereo in the standard house were turned off in winter (ESM Fig. C-6c).

Estimated daily mean window heat gains in the cool home always exceeded those in the standard home (ESM Fig. C-6d). Window heat differences were smallest in December and January, the months with least solar irradiation (ESM Fig. C-5).
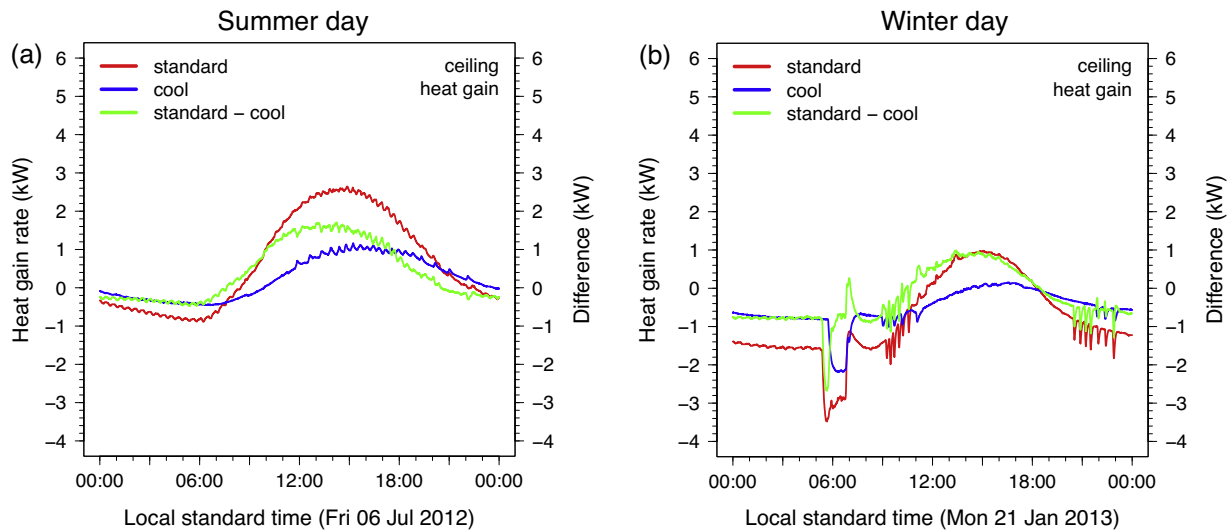
Fig. 5. Rates of ceiling heat gain on (a) the summer day and (b) the winter day.

Table 3
Seasonal mean reductions (standard − cool) in daily maximum and daily mean temperatures and heat gain rates.

	Cooling season (May–October)		Heating season (November–April)	
	Max	Mean	Max	Mean
Roof top temperature (°C)	13.0	3.4	10.8	1.7
Roof bottom temperature (°C)	13.5	3.7	10.2	1.9
Attic air temperature (°C)	9.8	2.4	6.9	1.0
Ceiling heat gain rate (W)	1370	311	805	−46
Duct heat gain rate (W)	819	129	0	−32
Ceiling + duct heat gain rate (W)	2190	440	805	−78

4.4. Daily and cumulative energy savings in the cooling and heating seasons

Fig. 7 shows in each season (cooling, heating) the daily and cumulative values of cool-roof energy savings per unit ceiling area.[3]

In the cooling season, Method A reports ceiling and duct heat gain savings divided by COP, while Method B subtracts from HVAC (compressor plus fan) electricity savings the difference (standard − cool) in plug load and window heat gains divided by COP. Cool-roof energy savings are assumed to be zero on days when HVAC systems are off in both homes. Method A and Method B agree well in the cooling season, with an especially close match from May through July (Fig. 7a,b). Cumulative cooling energy predicted by Method A (2.89 kWh/m^2) are 2% higher than those calculated from Method B (2.82 kWh/m^2) (Fig. 7b), which is very close.

Fig. 8 compares Method A and Method B daily energy savings for each day and each week of the cooling season. Agreement is especially good on a weekly basis.

In the heating season, the Method A formula switches sign, since the HVAC supplies, rather than removes, heat [Eq. (17)], while Method B *adds* to fuel savings the difference in plug load and window heat gains divided by AFUE. Method A over-predicts Method B in the heating season, especially from November through January (Fig. 7c,d). Cumulative heating fuel energy savings from Method A (3.34 kWh/m^2) are three times greater than those from Method B (1.13 kWh/m^2) (Fig. 7d).

Fig. 9 shows per unit ceiling area the daily and cumulative values of cool-roof fan energy savings in the heating season. For each

method (A and B), cool-roof fan energy savings are estimated by scaling daily fan energy savings by the ratio of cool-roof heating fuel energy savings to raw heating fuel energy savings. Cumulative heating-season cool-roof fan energy savings from Method A (0.077 kWh/m^2) are 2.7 times higher than those from Method B (0.029 kWh/m^2).

Note that Methods A and B each yield *positive* fuel and fan energy savings in the heating season, which we attribute to the higher thermal capacitance of the tile roof.

4.5. Daily peak-hour cooling power demand reduction

Fig. 10 shows daily values of peak-hour cooling power demand reduction, calculated on each weekday in the cooling season (May through October) as the mean value of cool-roof power demand reduction from 12:00 to 18:00 LT (11:00–17:00 LST). The seasonal mean demand reduction predicted by Method A (1.06 W/m^2) is about 20% higher than that calculated by Method B (0.88 W/m^2).

4.6. Seasonal and annual cumulative conditioning site energy, source energy, energy cost, and emission savings

Table 4 summarizes Method A and Method B values of seasonal and annual site energy, source energy, energy cost, and emission savings, all per unit ceiling area. Since the earlier analysis showed substantial differences in heating-season fuel and fan energy savings, the following reports the more conservative Method B savings, which are based on measured energy savings adjusted for measured differences in plug load heat gain and estimated differences in window heat gain. Each parenthetical value is relative to use, cost, or emission in the standard home.

---

[3] "Ceiling area" means the area of the ceiling on the top floor of the building.
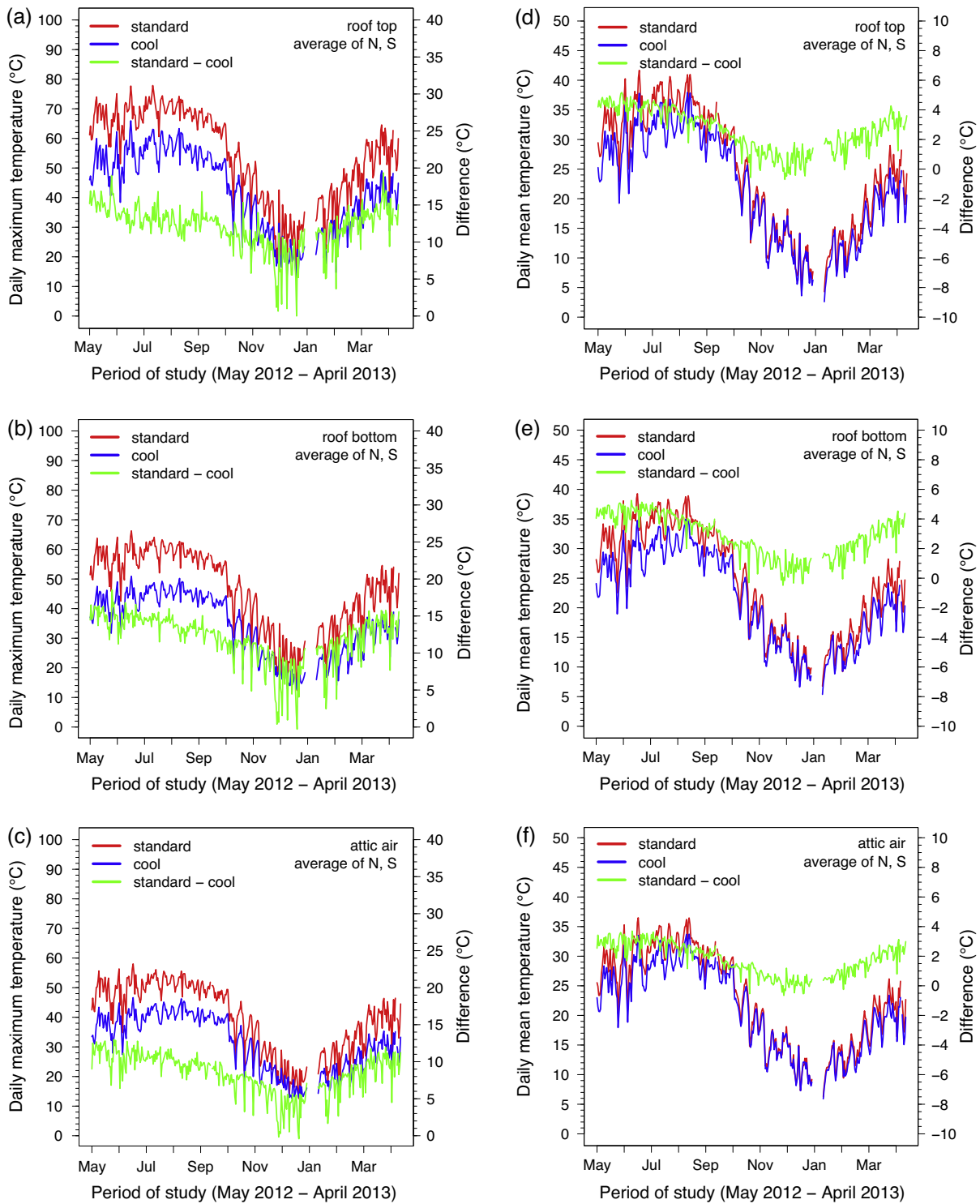
Fig. 6. Daily (a–c) maximum and (d–f) mean temperatures at roof top, roof bottom, and attic air.

- Annual cooling (compressor + fan) site energy savings are 2.82 kWh/m^2 (26%).
- Annual heating (furnace) fuel site energy savings are 1.13 kWh/m^2 [0.0386 therm/m^2] (4%).
- Annual heating (furnace) fan site energy savings are 0.0294 kWh/m^2 (3%).
- Annual conditioning (cooling + heating) source energy savings are 10.7 kWh/m^2 (15%).
- Annual conditioning energy cost savings are $0.886/m^2 (20%).

- Annual conditioning CO_2 emission reduction is 1.63 kg/m^2 (15%).
- Annual conditioning NO_x emission reduction is 0.621 g/m^2 (10%).
- Annual conditioning SO_2 emission reduction is 0.0462 g/m^2 (22%).
- Peak-hour cooling (compressor + fan) power demand reduction is 0.88 W/m^2 (37%).

Using the mean ceiling area of the two homes in this study (188 m^2), annual cooling, heating fuel, and heating fan site energy
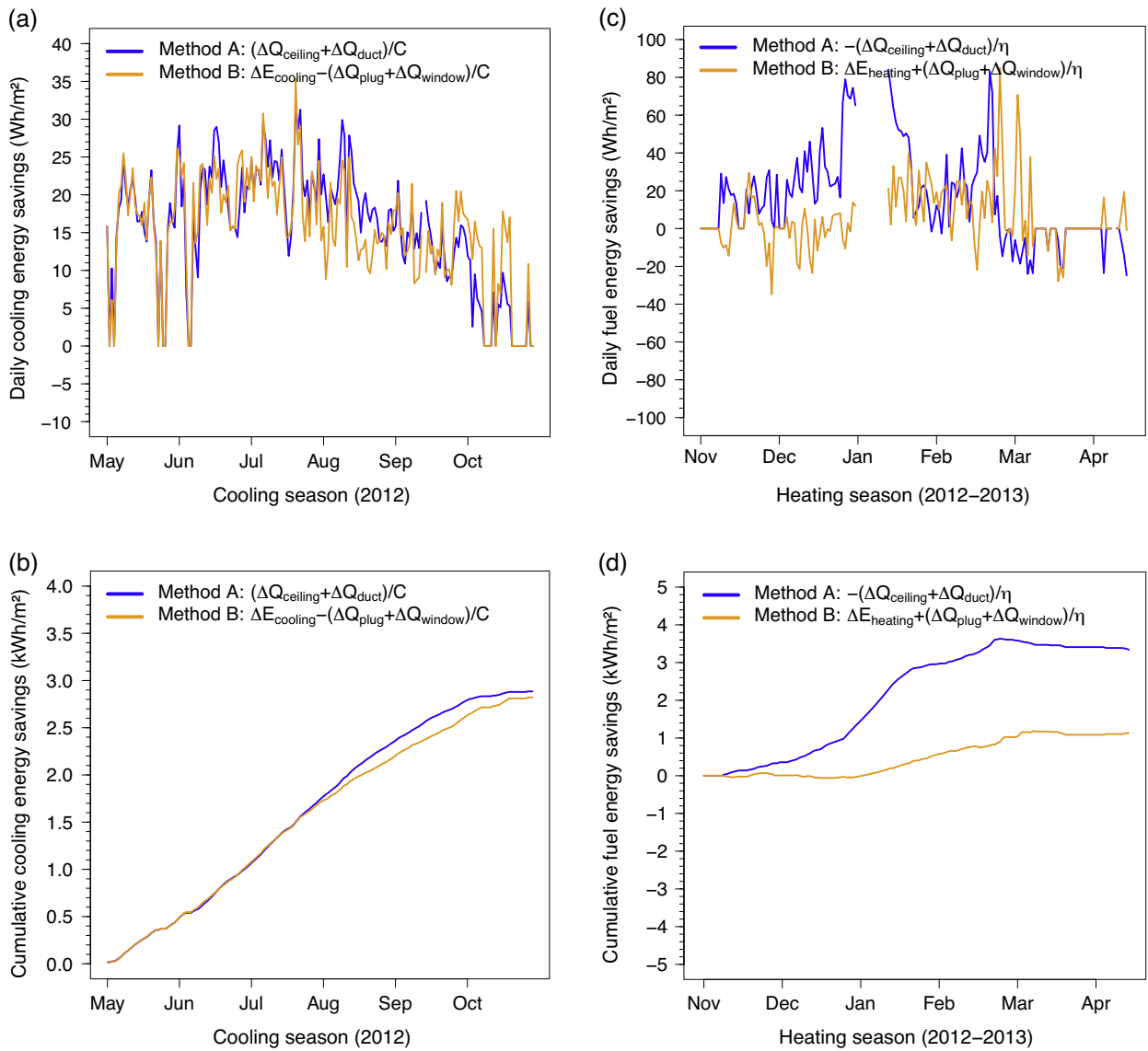
Fig. 7. Values per unit ceiling area of (a) daily and (b) cumulative cooling (compressor + fan) energy savings in the cooling season; and (c) daily and (d) cumulative fuel energy savings in the heating season.
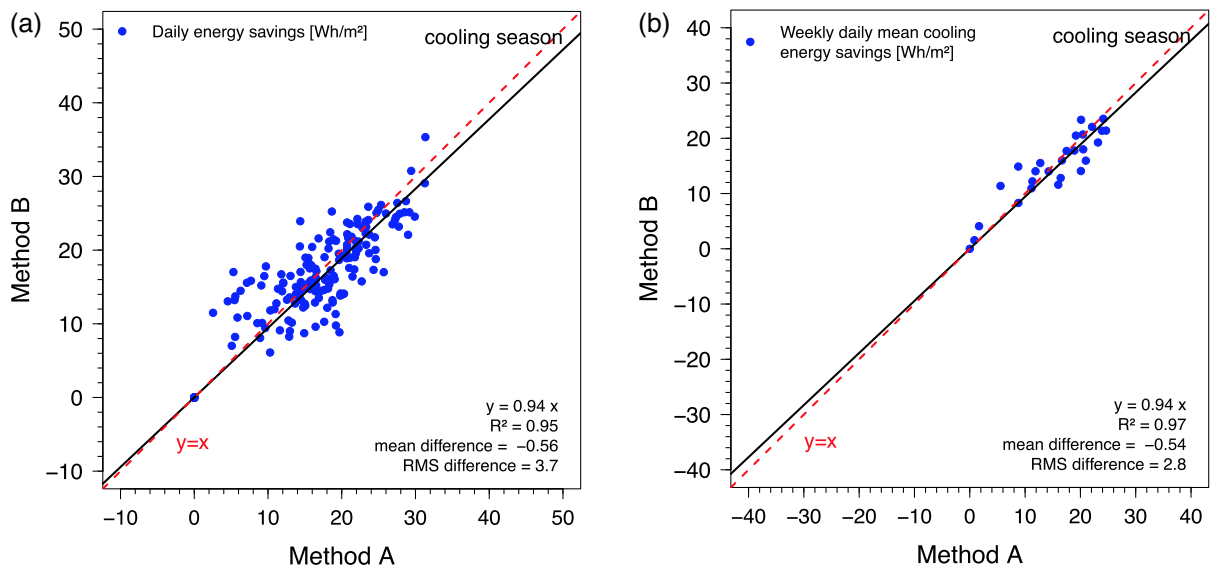

Fig. 8. Cooling season comparisons of Method A and Method B estimates of (a) daily and (b) weekly mean values of daily cool-roof energy savings per unit ceiling area.

(a)

Fig. 10. Daily peak-hour cooling power demand reduction in the cooling season.

5. Discussion

5.1. Cooling and heating energy savings

Following Method B, the cool home with the reflective tile roof (initial SR 0.51; thermal capacitance 40 kJ/m²·K) used 26% less annual cooling (compressor + fan) energy, 4% less annual heating fuel energy, and 3% less annual heating fan energy than the standard home with the dark shingle roof (initial SR 0.07; thermal capacitance 22 kJ/m²·K).

The Fresno home's fractional annual cooling energy savings (26%) were 2.6 times the 10% daily cooling energy savings that Parker and Barkaszi [18] measured after applying a white coating to an RSI-3.3 asphalt shingle roof on a Palm Bay, Florida home, even though (a) all three homes (Fresno cool, Fresno standard, Palm Bay) had RSI-3.3 attic insulation; (b) the roof albedo increase in Fresno (0.44) was the same as that in Palm Bay; and (c) based on the TMY3 typical meteorological year, the cooling-season (May–October) mean global horizontal solar irradiance in Fresno is only about 25% greater than that in Melbourne, FL (near Palm Bay) [42]. Similarly, fractional peak-hour cooling power demand savings in Fresno were 37%, or 2.3 times the 16% savings measured in Palm Bay at 17:00–18:00 LT.

While this study was not designed to isolate the effects of increasing roof thermal mass and adding above-sheathing ventilation from those of increasing roof albedo, some remarks can be made. First, basic physics suggests (a) that increasing roof albedo will tend to decrease roof temperature during the day
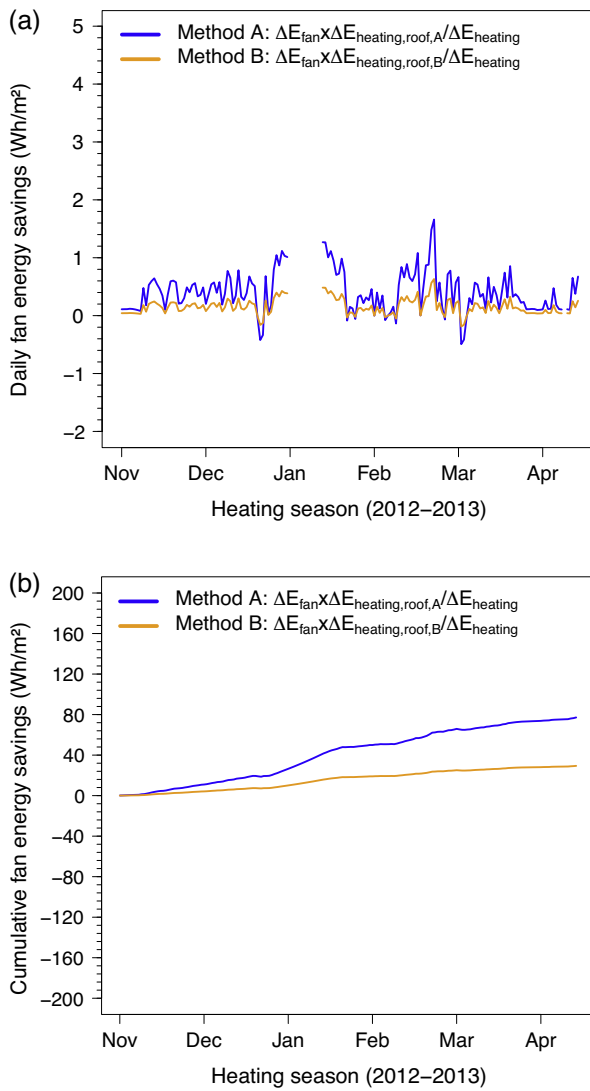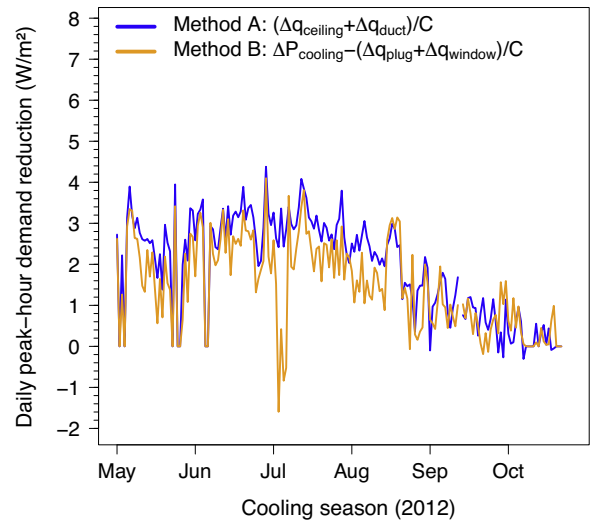
(b)

Fig. 9. Values per unit ceiling area of (a) daily and (b) cumulative fan energy savings in the heating season.

savings were 530 kWh, 212 kWh (7.25 therm), and 5.53 kWh, respectively. Annual conditioning source energy savings were 2010 kWh; annual energy cost savings were $167. Emission reductions were 307 kg CO_2, 117 g NO_x, and 8.69 g SO_2; peak-hour power demand reduction was 165 W.

Table 4
Daily, seasonal, and annual mean values of energy savings, energy cost savings, emission reduction, and peak-hour demand reduction per unit ceiling area. Method B fractional savings (relative to the standard house) are shown in parentheses.

Savings per unit ceiling area	Cooling season (May–October)		Heating season (November–April)		Annual	
	Method A	Method B	Method A	Method B	Method A	Method B
Daily site cooling energy (Wh/m²)	15.7	15.3				
Daily site heating fuel energy (Wh/m²)			18.5	6.24		
Daily site heating fan energy (Wh/m²)			0.426	0.162		
Seasonal or annual site electrical energy (kWh/m²)	2.89	2.82 (26%)	0.0772	0.0294 (3%)	2.97	2.85
Seasonal or annual site fuel energy (kWh/m²)	0.00	0.00	3.34	1.13 (4%)	3.34	1.13
Seasonal or annual source energy (kWh/m²)	9.65	9.42	3.76	1.28	13.4	10.7 (15%)
Seasonal or annual conditioning energy cost ($/m²)	0.861	0.840	0.131	0.0454	0.993	0.886 (20%)
Seasonal or annual CO_2 (kg/m²)	1.45	1.41	0.641	0.218	2.09	1.63 (15%)
Seasonal or annual NO_x (g/m²)	0.468	0.456	0.484	0.164	0.95	0.621 (10%)
Seasonal or annual SO_2 (g/m²)	0.0459	0.0448	0.00419	0.00147	0.0501	0.0462 (22%)
Peak-hour site electrical demand (W/m²)	1.06	0.88 (37%)				

(sunny), while minimally affecting that at night (no sun); (b) above-sheathing ventilation enhances roof heat transfer mostly during the day, because buoyant air flow in the space between the sheathing and roofing is driven by the temperature difference between roof and outside air; and (c) increasing roof thermal mass will tend to lower roof temperature during the day and raise it at night by slowing temperature change. On the representative summer day, the magnitude of the maximum roof bottom temperature difference (standard – cool), around 12:00 LST, was over five times greater than that of the minimum roof bottom temperature difference, near 00:00 LST (Fig. 4c). Similarly, on that day the magnitude of the maximum ceiling heat gain difference (standard – cool), around 14:00 LST, was over four times greater than that of the minimum ceiling heat gain difference, near 06:00 LST (Fig. 5a). This indicates that daytime reductions in roof temperature and/or ceiling heat flux resulted predominantly from raising albedo and adding above-sheathing ventilation, rather than from increased thermal storage.

Second, while the tile roof's higher thermal mass (80% greater than that of the shingle roof) delayed peak ceiling + duct heat gain by about an hour (ESM Table C-3), this shift may not have substantially reduced summer cooling loads, because the cool home's AC operated well into the evening (ESM Fig. C-7a). Thus, the improved fractional cooling energy savings (26% vs. 10%) and fractional peak demand reduction (37% vs. 16%) observed in Fresno likely resulted from the tile roof's above-sheathing ventilation (1.9–4.4 cm air gap below tiles; none below shingles), rather than its higher thermal mass. These boosts in savings are qualitatively consistent with the 50% ceiling heat flux reduction measured by Miller and Kosny [24] when comparing an SR 0.13 flat tile roof on double battens to an SR 0.09 shingle roof.

Third, the slightly positive fractional annual heating energy savings in Fresno (4%) differs in sign from the fractional annual heating energy savings (e.g., −5% in Los Angeles; −2% in Phoenix) simulated by Akbari et al. [3] for a 0.30 increase in the albedo of an RSI-3.3 asphalt shingle roof. Here the improvement likely results from the tile roof's high thermal capacitance, which increases the overnight temperature of the attic air.

5.2. Importance of corrections to measured energy savings

ESM Fig. C-6 shows that differences (standard – cool) in daily mean rates of ceiling, plug load, duct, and window heat gain were generally comparable in magnitude (−0.5 kW to +0.5 kW). This confirms the importance of correcting measured HVAC savings for differences in window and plug load heat gain, as shown in the Method-B Eqs. (20) and (21).

5.3. Estimating cooling energy savings from temperature and heat flux measurements

The close agreement between Methods A and B in the cooling season suggest that Method A can be used to estimate cooling energy savings without measuring HVAC or plug load power demand. A minimalist and quite economical *cooling season* experiment would require in each building only seven temperature sensors—roof top, attic air, room air, supply duct inlet, supply duct outlet, return duct inlet, and return duct outlet—and one ceiling heat flux sensor. While not strictly needed to measure energy savings, multiple roof top temperature sensors would be warranted if the roof is not flat.

If the HVAC's cooling COP and fan-on air flow rate are known from equipment specifications, duct heat gain rate and Method A cooling power savings can be computed from Eqs. (4) and (18), respectively. For calculation of duct heat gain rate, the fan can be assumed on if the supply duct outlet air temperature is far from the room air temperature, and off otherwise.

Methods A and B each reference the heating and cooling COPs of the HVAC equipment. We note that the COP of an air conditioner or heat pump can vary with load factor, outside air temperature, and refrigerant charge [47].

6. Summary

Temperatures, heat flows, and energy uses were measured for a year in two side-by-side, single-story, single-family homes in Fresno, California. One house had a reflective concrete tile roof (initial SR 0.51; thermal capacitance 40 kJ/m^2·K), and the other a standard dark asphalt shingle roof (initial SR 0.07; thermal capacitance 22 kJ/m^2·K). The flat tiles were mounted on battens, creating an air gap between tile and deck; the shingles were affixed directly to deck. The buildings were otherwise similar in construction and occupancy, with some differences in heat gains from plug loads and windows.

On a representative summer day (6 Jul 2012), maximum roof top, roof bottom, and attic air temperatures in the cool home (tile roof) were 13.8, 14.3, and 10.5 °C lower than in the standard house (shingle roof). Maximum rates of ceiling, duct, and ceiling + duct heat gain in the cool home were 1.50, 0.89, and 2.4 kW lower than in the standard house. Minimum roof top, roof bottom, and attic air temperatures in the cool roof home were 2.1, 2.4, and 2.4 °C *higher* than in the standard house, likely resulting from the higher thermal capacitance of the tile roof.

On a representative winter day (21 Jan 2013), maximum roof top, roof bottom, and attic air temperatures in the cool home were 11.0, 10.6, and 6.9 °C lower than in the standard house. Maximum ceiling, duct, and ceiling + duct rates of heat gain in the cool home were 0.83, 1.33, and 1.17 kW lower than in the standard house. Minimum roof top, roof bottom, and attic air temperatures in the cool home were 0.4, 2.1, and 2.3 °C *higher* than in the standard house.

The north and south side temperature measurements explored in Appendix B suggest that (a) as expected, it is important to measure roof top and roof bottom temperatures on all faces of a sloped roof; (b) while good practice, measuring attic air and attic floor temperatures at more than one point is not strictly necessary; and (c) attic floor temperature sensors should be placed away from supply registers.

In the cooling season (May–October), the mean rates of ceiling and duct heat gain in the standard home were about 310 W and 130 W lower in the cool home than in the standard home. However, mean rates of ceiling and duct heat gain in the heating season (November–April) were about 46 W and 32 W *greater* in the cool home than in the standard home, likely resulting from the higher thermal capacitance of the cool roof.

Seasonal mean reductions (standard – cool) in roof top, roof bottom, and attic air temperatures in the cooling season were about 3.4 °C, 3.7 °C, and 2.4 °C, roughly twice those the heating season. Above-sheathing ventilation cooling the deck of the cool tile roof may have made the temperature difference (standard – cool) at roof bottom (underside of roof deck) larger than that at roof top (just below tile surface).

Cool-roof energy savings in the cooling and heating seasons were computed two ways. Method A divides by the HVAC's COP the difference (standard – cool) in ceiling + duct heat gain. Method B measures the difference in HVAC energy use, corrected for differences in plug and window heat gains. Methods A and B agreed well in the cooling season, but not in the heating season. Therefore, all savings are reported based on Method B, which yielded more conservative savings in winter.

Relative to the standard home, annual cooling (compressor + fan), heating fuel, and heating fan energy savings at the site were 2.82 kWh/m^2 (26%), 1.13 kWh/m^2 (4%), and 0.0294 kWh/m^2 (3%), respectively. Annual conditioning source energy savings were

10.7 kWh/m^2 (15%); annual energy cost savings were \$0.886/m^2 (20%). Annual conditioning CO_2, NO_x, and SO_2 emission reductions were 1.63 kg/m^2 (15%), 0.621 g/m^2 (10%), and 0.0462 g/m^2 (22%). Peak-hour cooling (compressor + fan) power demand reduction was 0.88 W/m^2 (37%). For the studied homes with 188 m^2 ceilings, annual cooling, heating fuel, and heating fan site energy savings were 530 kWh, 212 kWh (7.25 therm), and 5.53 kWh, respectively. Annual conditioning source energy savings were 2010 kWh; annual energy cost savings were \$167. Emission reductions were 307 kg CO_2, 117 g NO_x, and 8.69 g SO_2; peak-hour power demand reduction was 165 W.

Fractional annual cooling energy savings (26%) were 2.6 times the 10% daily cooling energy savings measured in a previous study that used a white coating to increase the albedo of an asphalt shingle roof by the same amount (0.44). Fractional peak-hour cooling power demand savings (37%) were 2.3 times the 16% savings observed in the earlier study. The improved cooling energy savings (26% vs. 10%) may be attributed to the cool tile's above-sheathing ventilation, rather than to its high thermal mass.

The slightly positive fractional annual heating energy savings likely resulted from the tile roof's high thermal capacitance, which increased the overnight temperature of the attic air.

Acknowledgements

Appendix A. HVAC operation patterns

ESM Fig. C-7 shows HVAC fan power demand in the standard and cool houses on sunny summer and winter days. The difference (standard − cool) in attic air temperature is overlaid on each graph because difference in attic air temperature drives differences in ceiling and duct heat gains.

On the summer day, the HVAC systems (cooling) are completely off from about 22:30 LST (late night) to 11:30 LST (just before noon), and cycle on/off at other times. On the winter day, the HVAC systems (heating) are completely off from 23:00 LST (late at night) to 05:30–06:00 LST (early morning), from 07:00 to 09:00 LST (midmorning), and from 11:00 to 20:30–22:00 LST (late morning to late night), running continuously for about 1.5 h in the early morning and cycling on/off for another 4–5 h in the mid-morning and late evening.

The HVAC performance observed on the summer day supports the premise of including all hours of day when integrating cooling power savings, because the period of non-operation in which there is a substantial difference in attic air temperature (about 08:00–11:00 LST) is immediately followed by about 7 h of operation. The winter-day HVAC operation suggests that including all hours of day when integrating heating power savings may overestimate the heating energy penalty, because the primary heating period (early morning, following the nighttime setback of the thermostat) begins about 10 h after the attic air temperature difference falls to a small nighttime value.

Appendix B. Differences between north and south side building temperatures

On a clear summer day, the south face of the roof receives less direct solar irradiance than the north face in the early morning and early evening, but more in the middle of the day. On a clear winter day, the south face roof receives more direct irradiance throughout the day (see Section 3.3).

ESM Fig. C-8 shows the temperature differences between the south and north sides of the standard home on sunny summer and winter days. On the summer day, the difference (south − north) was about −5 to +6 °C at the roof top, −3 to +4 °C at the roof bottom, −1 to +1 °C at the attic air, and 0 to 2 °C at the attic floor.

On the winter day, roof top and roof bottom differences were much larger, ranging from −1 to +24 °C at the roof top and 0 to 13 °C at the roof bottom. Winter-day attic air temperature differences were close to zero. The south–north attic floor temperature differences on that day were up to 4 °C because the south-side attic floor temperature sensor was close to a supply register, while its north-side counterpart was not. (Proximity to a supply register has little effect on attic floor temperature in summer, when the cold supply air falls, but strong influence in winter, when the warm supply air rises.)

Similar results were observed in the cool home on the summer and winter days (ESM Fig. C-9).

The north and south side temperature measurements suggest that (a) as expected, it is important to measure roof top and roof bottom temperatures on all faces of a sloped roof; (b) while good practice, measuring attic air and attic floor temperatures at more than one point is not strictly necessary; and (c) attic floor temperature sensors should be placed away from supply registers.

Appendix C. Electronic supplementary material (ESM)

Supplementary material related to this article can be found, in the online version, at http://dx.doi.org/10.1016/j.enbuild.2014.04.024.

References

[1] EIA, Residential Energy Consumption Survey, US Energy Information Administration, 2011, http://www.eia.gov/consumption/residential/reports/2009/square-footage.cfm

[2] H. Akbari, Cool roofs save energy, ASHRAE Transactions 104 (1B) (1998) 783–788.

[3] H. Akbari, S. Konopacki, M. Pomerantz, Cooling energy savings potential of reflective roofs for residential and commercial buildings in the United States, Energy 24 (5) (1999) 391–407.

[4] H. Akbari, P. Berdahl, R. Levinson, S. Wiel, A. Desjarlais, W.A. Miller, N. Jenkins, A. Rosenfeld, C. Scruton, Cool colored roofs to save energy and improve air quality, in: Proceedings of the 2004 ACEEE Summer Study on Energy Efficiency in Buildings, August 22–27, 2004, http://www.osti.gov/scitech/biblio/860746

[5] S. Konopacki, H. Akbari, Simulated Impact of Roof Surface Solar Absorptance, Attic, and Duct Insulation on Cooling and Heating Energy Use in Single-family New Residential Buildings. Report LBNL-41834, Lawrence Berkeley National Laboratory, Berkeley, CA, 1998, http://eetd.lbl.gov/node/55863

[6] R. Levinson, H. Akbari, Potential benefits of cool roofs on commercial buildings: conserving energy, saving money, and reducing emission of greenhouse gases and air pollutants, Energy Efficiency 3 (1) (2010) 53–109.

[7] A. Synnefa, M. Santamouris, H. Akbari, Estimating the effect of using cool coatings on energy loads and thermal comfort in residential buildings in various climatic conditions, Energy and Buildings 39 (2007) 1167–1174.

[8] H. Akbari, S. Konopacki, Calculating energy-saving potentials of heat-island reduction strategies, Energy Policy 33 (2005) 721–756.

[9] R. Levinson, H. Akbari, S. Konopacki, S. Bretz, Inclusion of cool roofs in nonresidential Title 24 prescriptive requirements, Energy Policy 33 (2005) 151–170.

[10] H. Akbari, L.S. Rose, Urban surfaces and heat island mitigation potentials, Journal of the Human-Environmental System 11 (2008) 85–101.

[11] M. Santamouris, Cooling the cities—A review of reflective and green roof mitigation technologies to fight heat island and improve comfort in urban environments, Solar Energy 103 (2014) 682–703.

[12] H. Taha, Meso-urban meteorological and photochemical modeling of heat island mitigation, Atmospheric Environment 42 (38) (2008) 8795–8809.

[13] H. Taha, Urban surface modification as a potential ozone air-quality improvement strategy in California: a mesoscale modelling study, Boundary-Layer Meteorology 127 (2008) 219–239.

[14] H. Akbari, S. Menon, A. Rosenfeld, Global cooling: increasing world-wide urban albedos to offset CO_2, Climatic Change 94 (2009) 275–286.

[15] S. Menon, H. Akbari, S. Mahanama, I. Sednev, R. Levinson, Radiative forcing and temperature response to changes in urban albedos and associated CO_2 offsets, Environmental Research Letters 5 (2010), 014005 (11 pp.).

[16] D. Millstein, S. Menon, Regional climate consequences of large-scale cool roof and photovoltaic array deployment, Environmental Research Letters 6 (2011) 034001, (9 pp.). http://dx.doi.org/10.1088/1748-9326/6/3/034001

[17] H. Akbari, H.D. Matthews, D. Seto, The long-term effect of increasing the albedo of urban areas, Environmental Research Letters 7 (2) (2012) 024004.

[18] D. Parker, S. Barkaszi, Roof solar reflectance and cooling energy use: field research results from Florida, Energy and Buildings 25 (1997) 105–115.

[19] W.A. Miller, A. Desjarlais, P. Childs, J. Atchley, H. Akbari, R. Levinson, P. Berdahl, California Home Demonstrations Showcasing the Energy Savings of Tile, Painted Metal and Asphalt Shingle Roofs with Cool Color Pigments. Report CEC-500-2006-067-AT7, California Energy Commission, Sacramento, CA, 2006, http://www.energy.ca.gov/2006publications/CEC-500-2006-067/CEC-500-2006-067-AT7.PDF

[20] W. Miller, W. MacDonald, A. Desjarlais, J. Atchley, M. Keyhani, R. Olson, J. Vandewater, Experimental analysis of the natural convection effects observed within the closed cavity of tile roofs, in: RCI Foundation Conference, "Cool Roofs: Cutting Through the Glare," Atlanta, GA, May 12–13, 2005.

[21] D. Parker, J. Sonne, J. Sherwin, Comparative evaluation of the impact of roofing systems on residential cooling energy demand in Florida, in: Proceedings of 2002 ACEEE Summer Study on Energy Efficiency in Buildings, Teaming for Efficiency, August, 2002, http://www.aceee.org/files/proceedings/2002/data/index.htm

[22] D. Parker, J. Sherwin, Comparative summer attic thermal performance of six roof constructions, ASHRAE Transactions 104 (Part 2) (1998) 1084–1092.

[23] G. De With, N. Cherry, J. Haig, Thermal benefits of tiled roofs with above-sheathing ventilation, Journal of Building Physics 33 (2) (2009) 171–194.

[24] W. Miller, J. Kosny, Next generation roofs and attics for homes, in: 2008 ACEEE Summer Study on Energy Efficiency in Buildings, Pacific Grove, CA, 2008, http://www.eceee.org/library/conference_proceedings/ACEEE_buildings/2008/Panel_1/1_34

[25] W.A. Miller, M. Keyhani, T. Stovall, A. Youngquist, Natural convection heat transfer in roofs with above-sheathing ventilation, in: Proceedings of Thermal Performance of the Exterior Envelopes of Buildings X, Clearwater, FL, December, 2007, http://web.ornl.gov/sci/buildings/2012/2007%20B10%20papers/019_Miller.pdf

[26] M. Dodson, Residential market: the western steep-slope market, Western Roofing Insulation and Siding 30 (5) (September/October 2007), http://www.westernroofing.net/residential_market.htm

[27] M. Dodson, Reader survey & western market share, Western Roofing Insulation and Siding 36 (4) (July/August 2013), http://westernroofing.net/Survey.html

[28] H. Akbari, C. Wray, T. Xu, R. Levinson, Inclusion of Solar Reflectance and Thermal Emittance Prescriptive Requirements for Residential Roofs in Title 24. Draft report presented at the California Energy Commission Workshop on 2008 Building Energy Efficiency Standards, Sacramento, California, May 19, 2006, http://energy.ca.gov/title24/2008standards/prerulemaking/documents/2006-05-18_workshop/2006-05-17_RESIDENTIAL_ROOFS.PDF

[29] F. Incropera, D. DeWitt, Fundamentals of Heat and Mass Transfer, 5th ed., Wiley & Sons, 2002, Section 8.3.3: Internal flow.

[30] R. Hendron, C. Engebrecht, United States DOE Building America House Simulation Protocols (Revised October 2010). U.S. DOE Building Technologies Program, 2010, http://www.nrel.gov/docs/fy11osti/49246.pdf

[31] PG&E, Time of Use Pricing, Pacific Gas & Electric Company, 2013, http://www.pge.com/mybusiness/energysavingsrebates/timevaryingpricing/timeofusepricing

[32] ASTM, ASTM Standard C1549-09: Standard Test Method for Determining Solar Reflectance Near Ambient Temperature Using a Portable Solar Reflectometer, American Society for Testing and Materials, West Conshohocken, PA, 2010, http://www.astm.org/Standards/C1549.htm

[33] CRRC, Cool Roof Rating Council Rated Products Directory, 2012, Retrieved on 28 Sep. 2012 from http://coolroofs.org/products/search.php

[34] R. Levinson, H. Akbari, P. Berdahl, Measuring solar reflectance—Part I: defining a metric that accurately predicts solar heat gain, Solar Energy 84 (2010) 1717–1744.

[35] R. Levinson, H. Akbari, P. Berdahl, Measuring solar reflectance—Part II: review of practical methods, Solar Energy 84 (2010) 1745–1759.

[36] HUD, 2011 American Housing Survey. Table C-11-AO, U.S. Department of Housing and Urban Development, 2011, http://www.census.gov/housing/ahs/files/ahs11/National2011.xls

[37] NREL, Measurement and Instrumentation Data Center Solar Position and Intensity (MIDC SOLPOS) Calculator, National Renewable Energy Laboratory, Golden, CO, 2013, http://www.nrel.gov/midc/solpos/solpos.html

[38] Sustainable By Design, Window Heat Gain tool, Seattle, WA, 2009, http://susdesign.com/windowheatgain/

[39] LBNL, WINDOW version 6.3. Windows and Daylighting Group, Lawrence Berkeley National Laboratory, Berkeley, CA, 2013, http://windows.lbl.gov/software/window/window.html

[40] Weather Underground, Historical weather for Fresno, CA, 2013, http://www.wunderground.com/history/airport/KFAT/MonthlyHistory.html#calendar

[41] The Weather Channel, Daily averages for Fresno, CA, 2013, http://www.weather.com/weather/wxclimatology/daily/USCA0406?climoMonth=7

[42] NREL, National Solar Radiation Data Base, 1991–2005 Update: Typical Meteorological Year 3, National Renewable Energy Laboratory, Golden, CO, 2005, http://rredc.nrel.gov/solar/old_data/nsrdb/1991-2005/tmy3

[43] EPA, ENERGY STAR Performance Ratings Methodology for Incorporating Source Energy Use, March 2011, US Environmental Protection Agency, 2011, http://www.energystar.gov/ia/business/evaluate_performance/site_source.pdf

[44] PG&E, Gas and Electric Rates, Pacific Gas & Electric Company, 2013, http://www.pge.com/nots/rates/tariffs/rateinfo.shtml

[45] EPA, eGRID2012 Version 1.0 Year 2009 Summary Tables, April 2012, US Environmental Protection Agency, 2012, http://www.epa.gov/cleanenergy/documents/egridzips/eGRID2012V1_0_year09_SummaryTables.pdf

[46] EPA, Compilation of Air Pollutant Emission Factors. Volume I: Stationary Point and Area Source (AP 42, Fifth Edition), US Environmental Protection Agency, 2005, http://www.epa.gov/ttnchie1/ap42

[47] M. Farzad, D.L. O'Neal, System performance characteristics of an air conditioner over a range of charging conditions, International Journal of Refrigeration 14 (6) (1991) 321–328.